SPE 165991

A Multiple-Continuum Model for Simulation of Gas Production from Shale Gas Reservoirs

Ning Li, RIPED of PetroChina; Qiquan Ran, RIPED of PetroChina; Jianfang Li, SPE, RIPED of PetroChina; Jiangru Yuan, RIPED of PetroChina; Cong Wang, SPE, Colorado School of Mines; Yu-Shu Wu, SPE, Colorado School of Mines

This paper was prepared for presentation at the SPE Reservoir Characterisation and Simulation Conference and Exhibition held in Abu Dhabi, UAE, 16–18 September 2013.

Abstract

Gas production from unconventional shale gas reservoirs is controlled by multi-scaled fractures, i.e., hydraulic fractures, natural fracture, micro fractures, etc., as flow pathways. On the other hand, shale matrix provides the majority of shale gas storage of both free and adsorbed gas. In addition, field data show that there exists significant amount of micro fractures within low-permeable shale matrix and these micro fractures may connect to large, global-connected fracture network. However, these micro fractures have been either ignored or lumped into the "matrix block" in the current simulation models. In this paper, we present a physically based multiple-continuum concept to include both natural and micro fractures as well as low-permeability shale matrix. The multiple-continuum conceptual model implemented considers shale gas rock consisting of (1) globally connected natural fractures, (2) micro fractures locally connected between matrix and/or kerogen to global fractures, and (3) low-permeability shale rock matrix. Similar to the classic double-porosity concept, the global fracture continuum is responsible for global gas flow to hydraulic fractures or wells, while low-permeability shale matrix, providing main storage space, is locally connected to micro-fractures and interacting with globally connecting fractures. In addition, our model formulation also includes the following processes: (1) nonlinear adsorption/desorption effect, (2) Klinkenberg effect, (3) non-Darcy flow (at high flow rate and low flow rate), and (4) pressure-sensitive rock deformation. We use a hybrid modeling approach to describe different types of fractures, including hydraulic fractures, natural fracture network, and micro fractures. We will demonstrate model application to quantify flow behavior in fractured shale gas reservoirs.

Introduction

Unconventional gas resources from shale gas reservoirs have received great attention in the past decade and become the focus of the petroleum industry as well as energy resources worldwide. This is because primarily of (1) their large reserves worldwide with the potential to supply the world with sufficient energy for decades and hundreds of years; (2) technical advances for commercial development of these resources in the past two decades, as demonstrated in North America; and (3) general usefulness and cleanness, in terms of CO_2 emission of natural gas, when compared with other fossil fuels. As a result of improved horizontal drilling and multiple-stage hydraulic fracturing technologies, the progresses have been made towards commercial gas production from such unconventional reservoirs in the world.

Flow behavior in shale gas reservoirs is characterized by single-phase (gas) and/or two-phase (gas and water) flow and transport in extremely low-permeability, highly heterogeneous porous/fractured, and stress-sensitive rock. Compared with flow in conventional reservoirs, gas flow in ultra-low permeability shale gas reservoirs is subject to more nonlinear, coupled processes, including nonlinear adsorption/desorption, non-Darcy flow (at high flow rate and low flow rate), and strong rock-fluid interaction, and rock deformation within nanopores or micro-fractures, coexisting with complex flow geometry and multi-scaled heterogeneity. Therefore, quantifying flow in shale gas reservoirs has been a significant challenge and traditional Darcy law equilibrium approaches, for example, may not be in general applicable. Because of the low permeability and highly nonlinear or non-Darcy flow behavior in such shale rock, the traditional, Darcy's law based simulators will not be in general applicable or realistic to handling nonlinearity of the flow in shale gas reservoirs.

Many analyses and discussions have been provided on the characteristics of flow behavior in shale gas reservoirs in SPE papers (e.g., Javadpour et al. 2007; Blasingame, 2008; Javadpour, 2009; Wu et al. 2009; Cipolla et al. 2010; Moridis et al. 2010; Wu and Fackahroenphol, 2011; Sakhaee-Pour and Bryant, 2011; Shabro et al. 2011; Wu et al. 2012; Wu and Wang, 2012). In this paper, we summarize some of the more relevant findings and conclusions regarding flow mechanisms and

physical processes of gas flow and production in shale gas formations. In this paper, we present a physically based multiple-continuum concept to include both natural and micro fractures as well as low-permeability shale matrix. The multiple-continuum conceptual model implemented considers shale gas rock consisting of (1) globally connected natural fractures, (2) micro fractures locally connected between matrix and/or kerogen to global fractures, and (3) low-permeability shale rock matrix. Similar to the classic double-porosity concept, the global fracture continuum is responsible for global gas flow to hydraulic fractures or wells, while low-permeability shale matrix, providing main storage space, is locally connected to micro-fractures and interacting with globally connecting fractures. In addition, our model formulation also includes the following processes: (1) nonlinear adsorption/desorption effect, (2) Klinkenberg effect, (3) non-Darcy flow (at high flow rate and low flow rate), and (4) pressure-sensitive rock deformation. We use a hybrid modeling approach to describe different types of fractures, including hydraulic fractures, natural fracture network, and micro fractures. We will demonstrate model application to quantify flow behavior in fractured shale gas reservoirs.

Flow Model

A multiphase system of gas and water in a porous or fractured unconventional shale gas reservoir is assumed to be similar to the black oil model, composed of two phases: gaseous and aqueous phases. For simplicity, the gas and water components are assumed to be present only in their associated phases, and adsorbed gas is within the solid phase of rock. Each fluid phase flows in response to pressure, gravitational, and capillary forces according to the multiphase extension of Darcy law or several non-Darcy laws, discussed below. In an isothermal system containing two mass components, subject to flow and sorption, two mass-balance equations are needed to fully describe the system, as described in an arbitrary flow region of a porous or fractured domain for flow of phase β (β = g for gas and β = w for water),

$$\frac{\partial}{\partial t}(\phi S_\beta \rho_\beta + m_k) = -\nabla \bullet (\rho_\beta \mathbf{v}_\beta) + q_\beta \tag{1}$$

where ρ_β is the density of fluid β; $\mathbf{v}_\beta$ is the volumetric velocity vector of fluid β; S_β is the saturation of fluid β; φ is the effective porosity of formation; t is time; m_k is the adsorption or desorption term for gas component (k=g only) per unit volume of formation; and q_β is the sink/source term of phase (component) β per unit volume of formation,

The flow velocity in Eq. (1) will be evaluated (1) using the Darcy's law with Klinkenberg effects (for gas flow); and (2) using the nonlinear flow models to describe non-Darcy flow behavior (e.g., Wu, 2002). Specifically, $\mathbf{v}_\beta$ is the flow velocity (or volumetric flow rate) in Eq. (1), defined differently under different flow regimes or situations, as discussed in the following.

Darcy's Flow: When the Darcy's law is applicable, the velocity, $\mathbf{v}_\beta$, is defined as,

$$\mathbf{v}_\beta = -\frac{k k_{r\beta}}{\mu_\beta}\left(\nabla \Phi_\beta\right) \tag{2}$$

where k is the absolute permeability of the porous media, treated as a function of gas pressure with Klinkenberg effect accounted for; $k_{r\beta}$ is relative permeability to phase β, treated as a function of fluid saturation; μ_β is the viscosity of phase β as a function of pressure; and $\nabla \Phi_\beta$ is flow potential gradient, defined as,

$$\nabla \Phi_\beta = \left(\nabla P_\beta - \rho_\beta g \nabla D\right) \tag{3}$$

where P_β is the pressure of phase β; g is gravitational acceleration constant; and D is the depth from a datum.

Non-Darcy's Flow: In addition to multiphase Darcy flow, non-Darcy flow may also occur between and among the continua in shale gas reservoirs. The flow velocity, $\mathbf{v}_\beta$, for non-Darcy flow of each fluid may be described using the multiphase extension of the *Forchheimer* equation (e.g., Wu, 2002),

$$-\left(\nabla \Phi_\beta\right) = \frac{\mu_\beta}{k_{r\beta}} k\, \mathbf{v}_\beta + \beta_\beta \rho_\beta \mathbf{v}_\beta \left|\mathbf{v}_\beta\right| \tag{4}$$

where β_β is the effective non-Darcy flow coefficient with a unit m^{-1} for fluid β under multiphase flow conditions.

Adsorption and Desorption of Gas in Shale Reservoirs: Natural gas can be present as a free gas phase or as adsorbed gas on solids in pores. In shales, methane molecules are adsorbed mainly to the carbon-rich components, i.e. kerogen (Silin and Kneafsey, 2011). As observed, adsorbed mass of gas can provide significant fraction of gas reserves and recovery. As the pressure decreases with gas production from reservoirs, more adsorbed gas is released from solid to free gas phase, contributing to the total production. In our model, the mass of adsorbed gas in formation volume V is described (Alana, 2011; Silin and Kneafsey, 2011):

$$m_g(V) = \rho_K \rho_g f(p) \overline{S_k} V \tag{5}$$

where ρ_K is kerogen density, ρ_g is gas density at standard condition, $\overline{S_k}$ is the average volume relative of kerogen in bulk volume, $m_g(V)$ is the adsorbed gas mass in bulk formation volume V. In Eq. (5), $f(P)$ is the adsorption isotherm function.

If the adsorbed gas molecules form a thin layer on the solid surface, adsorption terms can be well represented by the Langmuir isotherm (Langmuir, 1916), which describes the dependency of adsorbed gas volume on pressure at constant temperature.

$$f(P) = \frac{V_L P_g}{P_g + P_L} \tag{6}$$

where, V_L is the Langmuir volume (the maximum adsorption capacity at a given temperature), and P_L is the Langmuir pressure (the pressure at which the adsorbed gas content is equal to $\frac{V_L}{2}$).

Klinkenberg Effect: In low-permeability formation or under low pressure condition, the Klinkenberg effect (Klinkenberg, 1941) may be too significant to be ignored when modeling gas flow in reservoirs (Wu et al. 1998). Klinkenberg effect is expected to be larger in unconventional reservoirs, because of small size pores and low permeability associated. Under such flow conditions, absolute permeability for the gas phase is written as a function of gas pressure as,

$$k_g = k_\infty \left(1 + \frac{b}{P_g}\right) \tag{7}$$

where k_∞ is constant, absolute gas-phase permeability under very large gas-phase pressure (where the Klinkenberg effect is minimized); and b is the Klinkenberg factor, depending on the pore structure of the medium and formation temperature.

Coupled Flow and Geomechanics Effect: In this section, we will propose a very practical modeling approach, easily to implement to an existing reservoir simulator, to couple geomechanics with two-phase flow in unconventional reservoirs. Based on the observation from experimental results (e.g., Zeng et al. 2010; Lei et at. 2008; Wu et al. 2008; Winterfeld and Wu, 2011; 2012a; 2012b) and the previous research (e.g., Terzaghi, 1943; Rutqvist et al. 2002), the effective porosity, permeability, and capillary pressure of rock are assumed to correlate with the mean effective stress defined as,

$$\sigma'_m = \sigma_m(x, y, z, P) - \alpha P \tag{8}$$

where α is the Biot constant and

$$\sigma_m(x,y,z,P) = (\sigma_x(x,y,z,P) + \sigma_y(x,y,z,P) + \sigma_z(x,y,z,P))/3 \tag{9}$$

where σ_x, σ_y, and σ_z are total stress in x, y, and z- directions, respectively. With the definition of the mean effective stress in Equation (8), the effective porosity of formation (fractures or porous media) is defined as a function of mean effective stress only,

$$\phi = \phi(\sigma'_m) \tag{10}$$

Similarly, the intrinsic permeability is related to the effective stress, i.e.,

$$k = k(\sigma'_m) \tag{11}$$

For capillary-pressure functions, the impact of rock-deformation or pore-change is accounted for using the Leverett function (Leverett, 1941),

$$P_c = C_p P_c^0 (S_w) \frac{\sqrt{k^0/\phi^0}}{\sqrt{k(\sigma'_m)/\phi(\sigma'_m)}} \tag{12}$$

where P_c is the capillary pressure between gas and water as a function of water or gas saturation; C_p is a constant; and the superscript 0 denotes reference or zero-stress condition.

Several correlations have been used for porosity as a function of effective stress and permeability as a function of porosity (Winterfeld and Wu, 2011 and 2012a). Rutqvist et al. (2002) present the following function for porosity, obtained from laboratory experiments on sedimentary rock (Davies and Davies, 1999),

$$\phi = \phi_r + (\phi_0 - \phi_r) e^{-a\sigma'} \tag{13}$$

where ϕ_0 is zero effective stress porosity; ϕ_r is high effective stress porosity, and the exponent a is a parameter. They also present an associated function for permeability in terms of porosity,

$$k = k e^{c(\phi/\phi_0 - 1)} \tag{14}$$

where c is a parameter.

Numerical Model

As discussed above, the PDE that governs gas flow in gas reservoirs is nonlinear. In addition, gas flow in unconventional shale gas reservoirs is subject to many other nonlinear flow processes. In general, the flow model is solved using a numerical approach. This work follows the methodology for reservoir simulation, i.e., using numerical approaches to simulate gas and water flow, following three steps: (a) spatial discretization of mass conservation equations; (b) time discretization; and (c) iterative approaches to solve the resulting nonlinear, discrete algebraic equations.

Discrete Equations: The component mass-balance Equations (Eq.1) are discretized in space using a control-volume or integrated finite difference concept (Pruess et at. 1999), as shown in **Fig. 1**. The control-volume approach provides a general spatial discretization scheme that can represent a one-, two- or three-dimensional domain using a set of discrete meshes. Each mesh has a certain control volume for a proper averaging or interpolation of flow and transport properties or thermodynamic variables. Time discretization is carried out using a backward, first-order, fully implicit finite-difference scheme. The discrete nonlinear equations for components of gas and water at gridblock or node i can be written in a general form:

$$\left\{M_i^{k,n+1} + m_i^{k,n+1} - M_i^{k,n} - m_i^{k,n}\right\}\frac{V_i}{\Delta t} = \sum_{j\in\eta_i} flow_{ij}^{k,n+1} + Q_i^{k,n+1} \tag{15}$$

$$(k = 1, 2) \text{ and } (i=1, 2, 3, \ldots, N)$$

where superscript k serves also as an equation index for gas and water components with k = 1 (gas) and 2 (water); superscript n denotes the previous time level, with n+1 the current time level to be solved; subscript i refers to the index of gridblock or node i, with N being the total number of nodes in the grid; Δt is time step size; V_i is the volume of node i; η_i contains the set of direct neighboring nodes (j) of node i; M_i^k, m_i^k, $flow_{ij}^k$, and Q_i^k are the accumulation and reaction (absorption or desorption) terms, respectively, at node i; the component mass "flow" term between nodes i and j, and sink/source term at node i for component k, respectively, defined below.

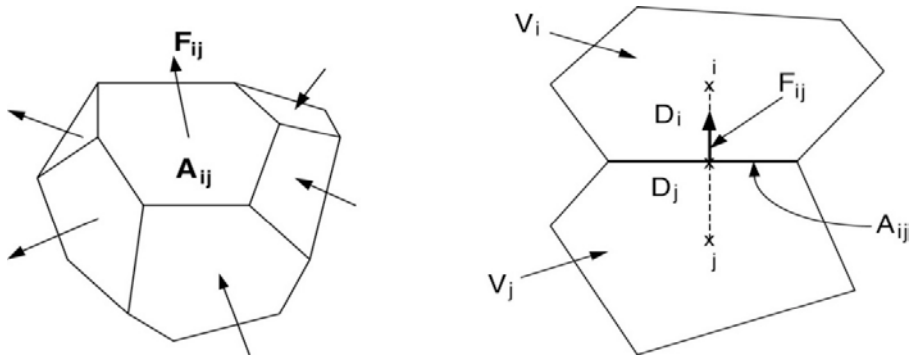

Fig. 1 Space discretization and flow-term evaluation in the integral finite difference method (Pruess et al. 1999)

The "flow" terms in Eq. (15) are mass fluxes by advective processes and are described by a discrete version of Darcy's law, i.e., the mass flux of fluid phase β along the connection is given by

$$\text{flow}_{\beta,ij} = \lambda_{\beta,ij+1/2}\gamma_{ij}\left(\Phi_{\beta j} - \Phi_{\beta i}\right) \tag{16}$$

where $\lambda_{\beta,i\,j+1/2}$ is the mobility term to phase β, defined as

$$\lambda_{\beta,i\,j+1/2} = \left(\frac{\rho_\beta k_{r\beta}}{\mu_\beta}\right)_{ij+1/2} \tag{17}$$

In Eq. (16), γ_{ij} is transmissivity and is defined as (Pruess et al. 1999),

$$\gamma_{ij} = \frac{A_{ij}k_{i\,j+1/2}}{D_i + D_j} \tag{18}$$

where A_{ij} is the common interface area between the connected blocks or nodes i and j (**Fig. 1**); D_i is the distance from the center of block i to the common interface of blocks i and j; and $k_{ij+1/2}$ is an averaged (such as harmonic-weighted) absolute permeability along the connection between elements i and j. The flow potential term in Eq. (16) is defined as,

$$\Phi_{\beta i} = P_{\beta i} - \rho_{\beta,ij+1/2}\, g\, Z_i \tag{19}$$

where Z_i is the depth to the center of block i from a reference datum.

Handling fractured media: to implement fractured modeling approaches, special attention is needed to calculate fracture-matrix mass transfer. Commonly used double-porosity (Warren and Root, 1963) and dual-permeability models use a quasi-steady state assumption for handling fracture-matrix interaction. In this work, the flow between fractures and matrix is still evaluated using Eq. (16); however, the transmissibility for the fracture-matrix flow is given by,

$$\gamma_{ij} = \frac{A_{Fm}k_m}{l_{Fm}} \tag{20}$$

where A_{Fm} is the total interface area between fractures and matrix of element i and j (one of them is a fracture and the other is a matrix blocks); k_m is matrix absolute permeability; and l_{Fm} is a characteristic distance or equivalent length for flow between fracture and matrix blocks. It can be calculated from ideal one-, two, and three-dimensional rectangular matrix block under quasi-steady state flow.

Triple-continuum or small fracture model has been proposed in the Yucca Mountain modeling study (Wu et al. 2004), which may be particularly of interest to fractured shale gas reservoir simulation. The triple-porosity model is developed based on field observation of fractures along the underground tunnel walls reveals of the Yucca Mountain unsaturated zone that many many ‘‘small’’ fractures are observed to exist in the unsaturated tuffs of the site. Field-observed fracture data as well as their statistical analyses indicate a large number of small- to intermediate-scale fractures are connected only locally to fractures along global-flow paths and do not directly contribute to global flow. These small-scale fractures are large in numbers and significantly increase contact areas between fractures and matrix systems, which may potentially impact overall flow and transport processes.

To capture effects of small-scale fractures or mirco-fractures, the fracture–matrix shale system is conceptualized as consisting of a single porous-medium rock matrix and two types of fractures: (1) ‘‘large’’ globally connected fractures and (2) ‘‘small’’ or miscro fractures that are locally connected to the large fractures and the rock matrix. The triple-continuum method extends the dual-permeability concept by adding one more connection (via small fractures) between the large fractures and the matrix blocks. Note that fractures not directly connected with large fractures (i.e., fractures that are isolated within the matrix) are not considered part of the small fracture continuum in this model. Instead, these fractures are considered as part of the matrix continuum. Note that the triple-continuum model is not limited to the orthogonal idealization of the fracture systems (Wu et a. 2004). Irregular and stochastic distributions of small and large fractures can be handled using a similar approach to the MINC methodology, as long as the actual distribution patterns are known.

In principle, the triple-continuum model, like the dual-continuum approach, uses an ‘‘effective’’ porous medium to approximate the two types of fractures and the rock matrix, and considers the three continua to be spatially overlapped. Like other continuum approaches, the triple-continuum model relies on the assumption that approximate thermodynamic equilibrium exists (locally) within each of the three continua at all times at a given location. Based on the local equilibrium assumption, we can define thermodynamic variables, such as pressures, for each continuum.

Handling Klinkenberg effect: To include the Klinkenberg effect on gas flow, the absolute permeability to gas phase in (18) should be evaluated using Eq. (7) as a function of gas phase pressure.

Handling non-Darcy flow: Under the non-Darcy flow condition of Eq. (4), the flow term ($\mathrm{flow}_{\beta,ij}$) in Eq. (15) along the connection (i, j), between elements i and j, is numerically defined as (Wu, 2002),

$$\mathrm{flow}_{\beta,ij} = \frac{A_{ij}}{2\left(k\beta_\beta\right)_{ij+1/2}}\left\{-\frac{1}{\lambda_\beta}+\left[\left(\frac{1}{\lambda_\beta}\right)^2-\bar{\gamma}_{ij}\left(\Phi_{\beta j}-\Phi_{\beta i}\right)\right]^{1/2}\right\} \tag{21}$$

in which the non-Darcy flow transmissivity is defined as,

$$\bar{\gamma}_{ij} = \frac{4\left(k^2\rho_\beta\beta_\beta\right)_{ij+1/2}}{D_i + D_j} \tag{22}$$

In evaluating the “flow” terms in the above Eqs. (16)-(22), subscript ij+1/2 is used to denote a proper averaging or weighting of fluid flow properties at the interface or along the connection between two blocks or nodes i and j. The convention for the signs of flow terms is that flow from node j into node i is defined as “+” (positive) in calculating the flow terms.

Eq. (15) presents a precise form of the balance equation for each mass component of gas and water in a discrete form. It states that the rate of change in mass accumulation (plus adsorption or desorption, if existing) at a node over a time step is exactly balanced by inflow/outflow of mass and also by sink/source terms, when existing for the node. As long as all flow terms have the flow from node i to node j equal to and opposite to that of node j to node i for fluids, no mass will be lost or created in the formulation during the solution. Therefore, the discretization in Eq. (15) is conservative.

Numerical Solution

In this work, we use the fully implicit scheme to solve the discrete nonlinear Eq. (15) with a Newton iteration method. Let us write the discrete nonlinear equation, Eq. (15), in a residual form as,

$$R_i^{k,n+1} = \left\{M_i^{k,n+1} + m_i^{k,n+1} - M_i^{k,n} - m_i^{k,n}\right\}\frac{V_i}{\Delta t} - \sum_{j\in\eta_i}\mathrm{flow}_{ij}^{k,n+1} - Q_i^{k,n+1} = 0 \tag{23}$$

(k = 1, 2 ; i = 1, 2, 3, …, N).

Eq. (23) defines a set of 2×N coupled nonlinear equations that need to be solved for every balance equation of mass components, respectively. In general, two primary variables per node are needed to use the Newton iteration for the associated two equations per node. The primary variables selected are gas pressure and gas saturation. The rest of the dependent variables, such as relative permeability, capillary pressures, viscosity and densities, adsorption term, as well as nonselected pressures, and saturation,—are treated as secondary variables, which are calculated from selected primary variables.

In terms of the primary variables, the residual equation, Eq. (23), at a node i is regarded as a function of the primary variables at not only node i, but also at all its direct neighboring nodes j. The Newton iteration scheme gives rise to

$$\sum_m \frac{\partial R_i^{k,n+1}\left(x_{m,p}\right)}{\partial x_m}\left(\delta x_{m,p+1}\right) = -R_i^{k,n+1}\left(x_{m,p}\right) \tag{24}$$

where x_m is the primary variable m with m = 1 and 2, respectively, at node i and all its direct neighbors; p is the iteration level; and i =1, 2, 3, …, N. The primary variables in Eq. (23) need to be updated after each iteration,

$$x_{m,p+1} = x_{m,p} + \delta x_{m,p+1} \tag{25}$$

The Newton iteration process continues until the residuals $R_i^{k,n+1}$ or changes in the primary variables $\delta x_{m,p+1}$ over iteration are reduced below preset convergence tolerances.

Numerical methods are generally used to construct the Jacobian matrix for Eq. (24), as outlined in Forsyth et al. (1995). At each Newton iteration, Eq. (24) represents a system of (2×N) linearized algebraic equations with sparse matrices, which are solved by a linear equation solver.

Treatment of Initial and Boundary Conditions

A set of initial conditions is required to start a transient simulation, i.e., a complete set of primary variables need to be specified for every gridblock or node. A commonly used procedure for specifying initial conditions is equilibrium calculation or restart option, in which a complete set of initial conditions or primary unknowns is generated in a previous simulation, with proper boundary conditions described.

Dirichlet boundary conditions are handled with the “inactive cell” or “big-volume” method, as normally used in the TOUGH2 code (Pruess et al. 1999). In this method, a constant pressure/saturation node is specified as an inactive cell or with a huge volume, while keeping all the other geometric properties of the mesh unchanged. For flux or Neuman boundary conditions, and multilayered wells, a general procedure for handling such boundary conditions is discussed in Wu et al. (1996 and 2000).

Model Application

To demonstrate the usefulness of the proposed generalized multi-continuum modeling approach in modeling gas flow through shale gas reservoirs, we present an application example: transient gas flow in a triple-continuum medium with two-scaled (large and small) fractures. In these examples, we are concerned with gas flow towards one horizontal well and 5-staged hydraulic fracture system in a shale gas reservoir. The reservoir formation is at liquid-gas, two-phase condition, however, the liquid saturation is set at residual values as an immobile phase. This is a single-phase gas flow problem and is modeled by the two phase flow reservoir simulator. The immobile liquid flow is controlled by liquid relative permeability curves.

The grid for modeling the horizontal well and multi-grid hydraulic fractures is shown in **Fig. 2**. Fractures and matrix parameters used for the examples are given in **Tab. 1**. The basic conceptualization for triple-continuum approximation of large-fracture, small-fracture, and rock matrix systems are shown in **Fig. 3**.

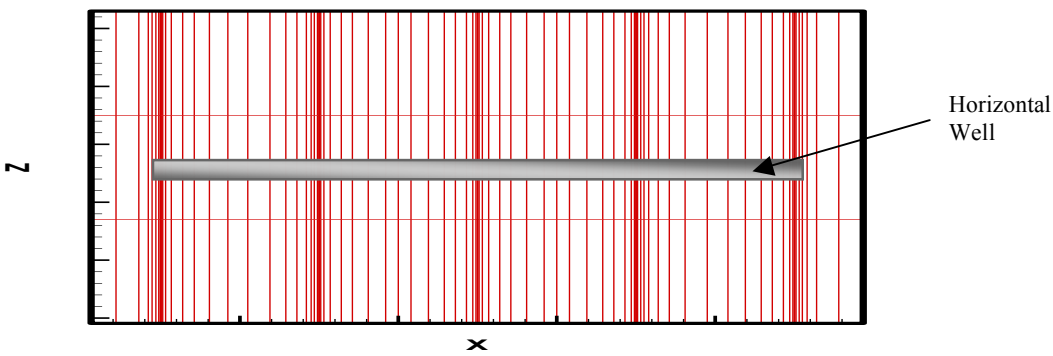

Fig. 2 Horizontal well and multi-grid hydraulic fracture

Tab. 1 Parameters used in the example

Parameter	Value	Unit	Parameter	Value	Unit
Reservoir length	△x=2,750	ft	Natural large-fracture spacing	A = 3.3	ft
Reservoir width	△y=2,000	ft	Natural small-fracture spacing	a = 0.7	ft
Formation thickness	△z=250	ft	F characteristic length	l_x = 1.6	ft
Horizontal well length	L_h=2,400	ft	F-f areas per unit volume rock	A_{Ff} = 65.6	ft^2/ft^3
Hydraulic fracture number	5	--	F-m areas per unit volume rock	A_{Ff} = 6.6	ft^2/ft^3
Distance between hydraulic fractures	y_e=200	ft	Matrix permeability	k_m=1.6E-02	md
Hydraulic fracture half-length	X_f=250	ft	Natural small-fracture permeability	k_{nsf}=1.0E+02	md
Reservoir depth	h=5,800	ft	Natural large-fracture permeability	k_{nlf}=1.0E+03	md
Reservoir temperature	T=200	F	Hydraulic fracture permeability	k_{hf}=1.0E+05	md
Initial reservoir pressure	P_i=3800	psi	Matrix porosity	ϕ_m = 0.05	--
Constant flowing bottomhole pressure	P_{wf}=500	psi	Natural small-fracture porosity	ϕ_{nsf} = 0.001	--
Viscosity	μ =0.0184	cp	Natural large-fracture porosity	ϕ_{nlf} = 0.004	--
Klinkenberg coefficient	b=200	psi	Hydraulic fracture porosity	ϕ_{hf} = 0.005	--
Non-darcy flow constant	c_β =3.2E-06	$m^{3/2}$	Matrix total compressibility	c_m=2.5E-04	psi^{-1}
Langmuir's pressure	P_L=2,285.7	psi	Natural fracture total compressibility	c_{nf}=2.5E-04	psi^{-1}
Langmuir's volume	V_L=218.57	scf/ton	Hydraulic fracture total compressibility	c_{hf}=2.5E-04	psi^{-1}

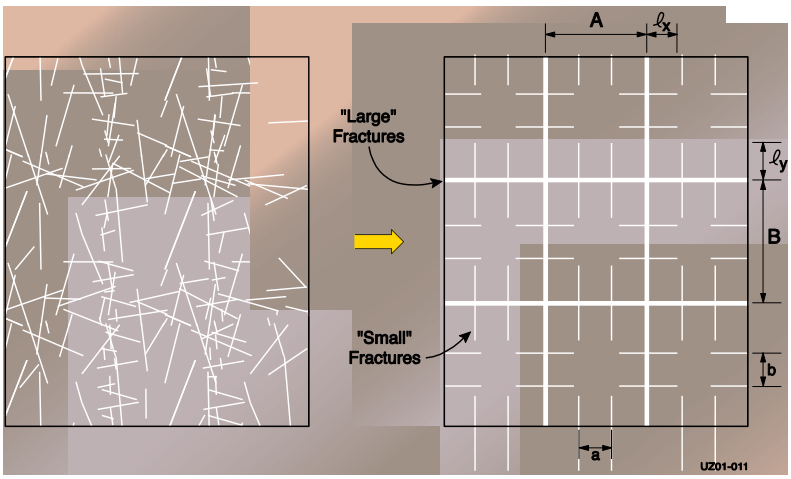

Fig. 3 Basic conceptualization for triple-continuum approximation of two-dimensional large-fracture, small-fracture, and rock matrix systems (Wu et al. 2004 and 2009)

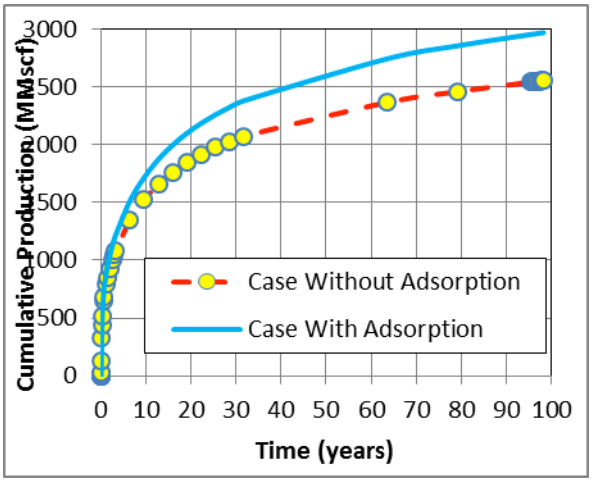

Fig. 4 Gas cumulative production behavior with Adsorption

Fig. 4 shows the results for well cumulative production versus time with and without Adsorption. The Adsorption causes obvious increase in cumulative production curve. The difference will become more and more evident. At t=100 years, the difference is 16.25% of cumulative production without considering any effects.

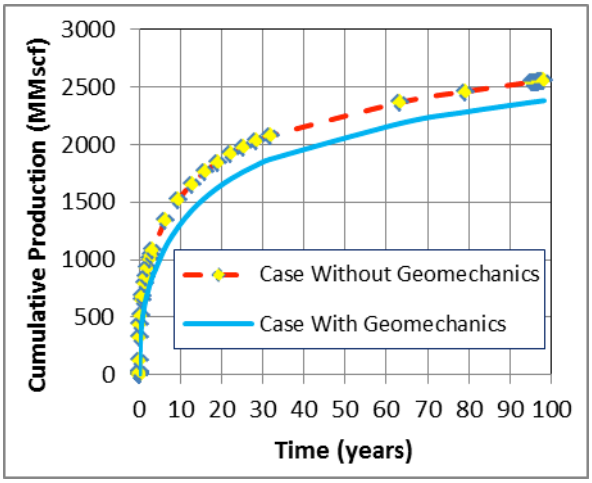

Fig. 5 Gas cumulative production behavior with Geomechanics

Fig. 5 shows the results for well cumulative production versus time with and without Geomechanics coupling effect. The Geomechanics coupling effect causes obvious decrease in cumulative production curve. The results illustrate that geomechanics-flow coupling has large impact on formation permeability especially for the natural fracture system.With the gas production, reservoir effective stress increases as pore pressure decreases, leading to the reduction of cumulative gas production. At t=100 years, the difference is ~6.83% of cumulative production without considering any effects.

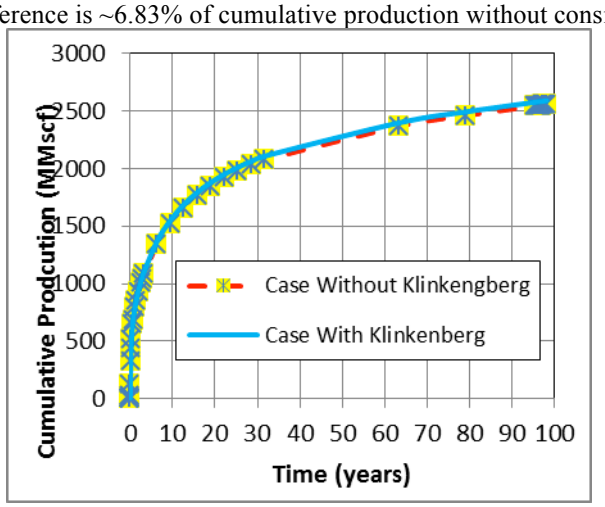

Fig. 6 Gas cumulative production behavior with Klinkenberg effect

Fig. 6 shows the simulated well cumulative production versus time with and without Klinkenberg effect. The Klinkenberg effect just causes small increase in cumulative production curve, which illustrates that the matrix permeability is increased a little. Becasue the matrix permeability is so small compared with natural fracture or hydraulic fracture permeability, this small change has little influence on the total production rate.

Fig. 7, 8, 9 and 10 present 4 cases results respectively, which include (a) comparison between with A(Adsorption)+ K (Klinkenberg effect) + G (Geomechanics) and without A+K+G (**Fig.7**); (b) comparison between with K+G and without K+G (**Fig.8**); (c) comparison between with A+K and without A+K (**Fig.9**); (d) comparison between with A+G and without A+G (**Fig.10**). The results show that the cumulative production increase 8.83% (with A+K+G), 17.82% (with A+K) and 7.61% (with A+G) respectively, and decrease ~5.8% (with K+G).

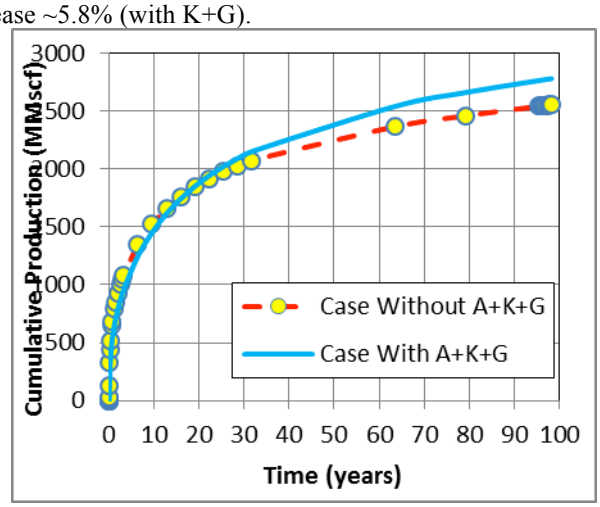

Fig. 7 Gas cumulative production behavior with Adsorption, Klinkenberg effect and Geomechanics

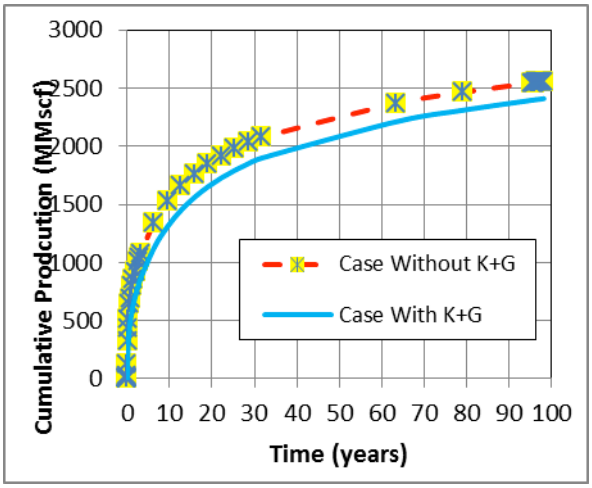

Fig. 8 Gas cumulative production behavior with Klinkenberg effect and Geomechanics

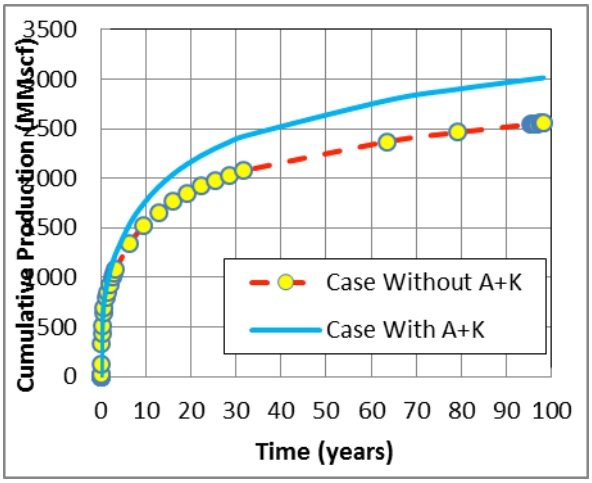

Fig. 9 Gas cumulative production behavior with Adsorption and Klinkenberg effect

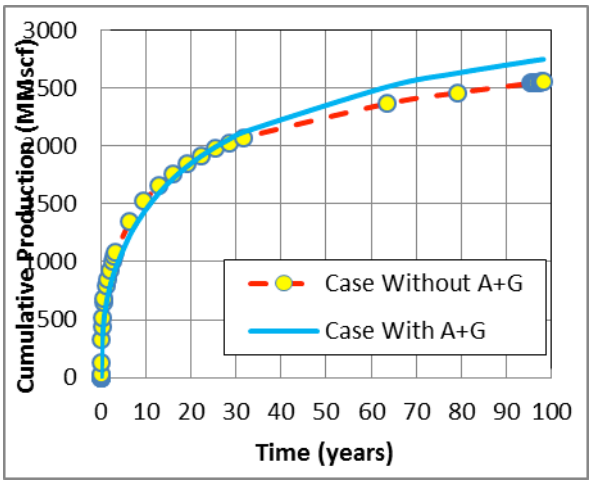

Fig. 10 Gas cumulative production behavior with Adsorption and Geomechanics

All in all, the sensitivity anaylsis results for Gas cumulative production are shown in **Fig. 11**. The results illustrate that adsorption is the most important positive effects in enhancing cumulative production of shale gas reservoir, and geomechanics is the most important negative effects in reducing cumulative production. The Klinkenberg effect has little influence to cumulative production in higher pressure. So, adsorption and geomechanics effects can not be neglected in shale gas reservoir.

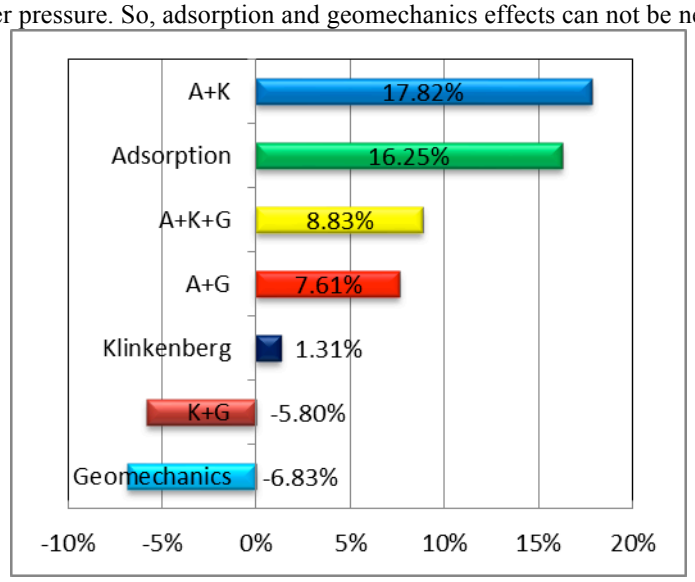

Fig. 11 The sensitivity anaylsis results for Gas cumulative production

Summary

In this paper, we present a multiple-continuum model for simulation of gas production from shale gas reservoirs. To describe gas flow behavior in such low-permeability, highly heterogeneous porous or fractured, and stress-sensitive rock, the model formulation incorporates many relevant physical processes, i.e., adsorption effect, Klinkenberg effect, non-Darcy flow with inertial effect, and coupled rock deformation and fluid flow. The numerical implementation of the unified formulation is based on a control-volume spatial discretization, using an unstructured grid, and the time discretized with a fully implicit finite-difference method. The final discrete linear or nonlinear equations are handled fully implicitly, using Newton iteration.

We present modeling studies using multiple-continuum model for gas production from a 5-staged hydraulic fractured horizontal well, incorporating adsorption effect, geomechanics effect, Klinkenberg effect and non-Darcy flow. The results illustrate that adsorption is the most important positive effects in enhancing cumulative production of shale gas reservoirs, and geomechanics has the most important negative effects on reducing cumulative production. The Klinkenberg effect has little influence to cumulative production in higher pressure. So, adsorption and geomechanics effects cannot be neglected in shale gas reservoir.

Acknowledgments

This work was supported by the National High Technology Research and Development Program of China (863 Program), "Typical Unconventional Reservoir Numerical Simulation Key Technology and Software Development 2013AA064902".

References

Blasingame, T.A., "The Characteristic Flow Behavior of Low-Permeability Reservoir Systems," SPE 114168, presented at the 2008 SPE Unconventional Reservoirs Conference held in Keystone, Colorado, U.S.A., 10–12 February 2008.

Cipolla, C.L., E.P. Lolon, J.C. Erdle, and B. Rubin, "Reservoir Modeling in Shale-Gas Reservoirs," *Reservoir Evaluation & Engineering*, August 2010.

Davies, J.P. and D.K. Davies, "Stress-Dependent Permeability Characterization and Modeling," SPE 56813, presented at SPE ATCE, Houston, TX, October 1999.

Forsyth, P. A., Y. S. Wu and K. Pruess, Robust numerical methods for saturated-unsaturated flow with dry initial conditions in heterogeneous media, *Advance in Water Resources,* 18, 25-38, 1955

Javadpour, F., "Nanopores and Apparent Permeability of Gas Flow in Mudrocks (Shales and Siltstone)," *Journal of Canadian Petroleum Technology,* V. 48, No. 8, August 2009.

Javadpour, F., D. Fisher, and M. Unsworth, "Nanoscale Gas Flow in Shale Gas Sediments," *Journal of Canadian Petroleum Technology*, V. 46, No.10, October 2007.

Klinkenberg, L.J., "The Permeability of Porous Media to Liquids and Gases," in API Drilling andProduction Practice, 200–213, 1941.

Langmuir, I., "The constitution and fundamental properties of solids and liquids," *Journal of the American Chemical Society*, 38 (11): 2221–2295, 1916.

Lei, Q. W. Xiong, J. Yuan, and Y.S. Wu, "Behavior of Flow through Low-Permeability Reservoirs," SPE 113144, presented at the 2008 SPE Europec/EAGE Annual Conference and Exhibition held in Rome, Italy, 9–12 June 2008.

Leverett, M.C., "Capillary Behavior in Porous Media," *Trans* AIME, 142:341-358, 1941.

Moridis, G.J., T.A. Blasingame, and C.M. Freeman, "Analysis of Mechanisms of Flow in Fractured Tight-Gas and Shale-Gas Reservoirs," SPE 139250, presented at the SPE Latin American & Caribbean Petroleum Engineering Conference held in Lima, Peru, 1–3 December 2010.

Pruess, K., C. Oldenburg and G. Moridis, *TOUGH2 User's Guide, Version 2.0,* Report LBNL-43134, Berkeley, California: Lawrence Berkeley National Laboratory, 1999.

Rutqvist, J. Y.S. Wu, C.F. Tsang, and G.S. Bodvarsson, "A Modeling Approach for Analysis of Coupled Multiphase Fluid Flow, Heat Transfer, and Deformation in Fractured Porous Rock," *International Journal of Rock Mechanics and Mining Sciences,* Vol. 39, 429-442, 2002.

Sakhaee-Pour, A. and S.L. Bryant, "Gas Permeability of Shale," SPE 146944, presented at the SPE Annual Technical Conference and Exhibition held in Denver, Colorado, USA, 30 October–2 November 2011.

Shabro, V., C. Torres-Verdín, and F. Javadpour, "Numerical Simulation of Shale-Gas Production: from Pore-Scale Modeling of Slip-Flow, Knudsen Diffusion, and Langmuir Desorption to Reservoir Modeling of Compressible Fluid," SPE 144355, presented at the SPE North American Unconventional Gas Conference and Exhibition held in The Woodlands, Texas, USA, 14–16 June 2011.

Silin, D. and T. Kneafsey, "Gas Shale: From Nanometer-scale Observations to Well Modeling," CSUG/SPE 149489, presented at the Canadian Unconventional Resources Conference, Calgary, Alberta, Canada, 15-17 November, 2011.

Terzaghi, K., *Theoretical Soil Mechanics*, John Wiley & Sons Inc., New York, 1943.

Warren, J. E., and P. J. Root, The behavior of naturally fractured reservoirs, *Soc. Pet. Eng. J.,* Trans., AIME, 228, 245-255, 1963.

Winterfeld, P. H. and Y.S. Wu, "A Novel Fully Coupled Thermal-Hydrologic-Mechanical Model for CO2 Sequestration in Brine Aquifers," submitted to and under review by International Journal of Rock Mechanics and Mining Sciences, 2012b.

Winterfeld, P. H. and Y.S. Wu, "A Novel Fully Coupled Geomechanical Model for CO2 Sequestration in Fractured and Porous Brine Aquifers," presented at the XIX International Conference on Water Resources CMWR 2012, University of Illinois at Urbana-Champagne June 17-22, 2012a.

Winterfeld, P. H. and Y.S. Wu, "Parallel Simulation of CO2 Sequestration with Rock Deformation in Saline Aquifers," SPE 141514, prepared for presentation at the SPE Reservoir Simulation Symposium held in The Woodlands, Texas, USA, 21–23 February 2011.

Wu, Y.S., C, Wang, J. Li, and P. Fackahroenphol, "Transient Gas Flow in Unconventional Gas Reservoirs," SPE-154448, presented at the EAGE Annual Conference & Exhibition incorporating SPE Europec held in Copenhagen, Denmark, 4–7 June 2012.

Wu, Y.S. and C. Wang, "Transient Pressure Testing Analysis of Gas Wells in Unconventional Reservoirs," SPE-SAS-312, presented at the 2012 SPE Annual Technical Symposium & Exhibition (ATS&E), Khobar, Saudi Arabia, 8-11 April 2012.

Wu, Y.S. and P. Fackahroenphol, "A Unified Mathematical Model for Unconventional Reservoir Simulation," SPE 142884, submitted for the SPE EUROPEC Conference, 23-26 May 2011 in Vienna, Austria, 2011.

Wu, Y.S. G. Moridis, B. Bai, and K. Zhang, "A Multi-Continuum Model for Gas Production in Tight Fractured Reservoirs," SPE 118944, Prepared for presentation at the 2009 SPE Hydraulic Fracturing Technology Conference held in The Woodlands, Texas, USA, 19–21 January 2009.

Wu, Y.S., J. Rutqvist, K. Karasaki, Q. Lei, W. Xiong, J. Yuan, M. Liu, and Y. Di, A Mathematic Model for Rock Deformation Effect of Flow in Porous and Fractured Reservoirs," presented at the 42nd US Rock Mechanics Symposium and 2nd U.S.-Canada Rock Mechanics Symposium, San Francisco, CA, 2008.

Wu, Y.S., H.H. Liu, and G.S. Bodvarsson, "A Triple-Continuum Approach for Modeling Flow and Transport Processes in Fractured Rock," *Journal of Contaminant Hydrology*, 73, pp.145-179, 2004.

Wu, Y.S., "Numerical Simulation of Single-Phase and Multiphase Non-Darcy Flow in Porous and Fractured Reservoirs," *Transport in Porous Media*, Vol. 49, No. 2, 209-240, 2002.

Wu, Y.S. A Virtual Node Method for Handling Wellbore Boundary Conditions in Modeling Multiphase Flow in Porous and Fractured Media, *Water Resources Research*, 36 (3), 807-814, 2000.

Wu, Y.S., K. Pruess, and P. Persoff, "Gas Flow in Porous Media with Klinkenberg Effects," *Transport in Porous Media*, Vol.32, 117-137, 1998.

Wu, Y.S., P.A. Forsyth and H. Jiang, A Consistent Approach for Applying Numerical Boundary Conditions for Subsurface Flow, *Journal of Contaminant Hydrology*, Vol. 23, 157-185, 1996.

Zeng, B., L. Cheng, and F. Hao, "Experiment and Mechanism Analysis on Threshold Pressure Gradient with Different Fluids," SPE 140678, Nigeria Annual International Conference and Exhibition, Tinapa - Calabar, Nigeria, 31 July - 7 August 2010.